Pergamon

CEMENT AND
CONCRETE
RESEARCH

Cement and Concrete Research 29 (1999) 503–506

Hydration of α'_{L}- and β-dicalcium silicates with identical concentration of phosphorus oxide

K. Fukuda *, H. Taguchi

Department of Materials Science and Engineering, Section of Inorganic Materials, Nagoya Institute of Technology, Gokiso-cho, Showa-ku,
Nagoya 466-8555, Japan

Manuscript received 29 June 1998; accepted manuscript 19 October 1998

Abstract

The hydration behavior of specimens with identical chemical compositions $(Ca_{1.955}\square_{0.045})(Si_{0.91}P_{0.09})O_4$ but different in phase compositions was examined. One composition was 30% α'_{L} and 70% β, whereas the other composition was 92% α'_{L} and 8% β. During the early stage of the hydration process of about 3 days, the specimen rich in the β-phase showed a much higher hydraulic activity than that rich in the α'_{L}-phase. Because these powder specimens showed almost the same specific surface areas and particle size distributions, the higher reactivity with water was ascribed to the more favorable defect state on the crystal surface. The β-phase showed polysynthetic twinning on $(100)_{\beta}$. The intersections of the twin boundaries and the crystal surface would behave like active centers of the reaction with water. The β-phase, therefore, showed a much higher cumulative heat for the 3-day curing than the α'_{L}-phase, the crystal fragments of which were nearly uniform with occasional line defects. After hydration for 15 days, both specimens showed almost the same cumulative heat of about 120 J/g. The heat evolution continued for 34 days, with the eventual cumulative heat of 143 ± 3 J/g. © 1999 Elsevier Science Ltd. All rights reserved.

Keywords: Ca_2SiO_4; Hydration; Crystal structure; Characterization

With Ca_2SiO_4 solid solutions (C_2S(ss)), the effects of polymorphism on hydration reactivity have been studied extensively [1–8]. However, the differences in reactivity between the β- and α'_{L}-phases have not yet been fully clarified. This is partly because the samples examined involved many variables, including chemical composition, which are difficult or thought to be impossible to control independently [9], and partly because there might be an uncertainty concerning the phase identification, especially for the "α'-phase."

High-temperature phase studies in the Ca_2SiO_4-$Ca_3(PO_4)_2$ system showed that Ca_2SiO_4 incorporates certain amounts of P_2O_5 [10–14]. When these crystals, $(Ca_{2-x/2}\square_{x/2})(Si_{1-x}P_x)O_4$, are quenched from elevated temperatures, however, they do not necessarily give exactly the same structures as the high-temperature modifications. They sometimes show modulated distortions with respect to the underlying othohexagonal α-phase structure [13,15–18]. The distinct incommensurate (INC) superstructure was obtained at ambient temperature for the crystals with $0.175 \leqslant x \leqslant 0.225$ [18]. This phase often has been misidentified as the α'-phase due to the similarity in powder X-ray diffraction (XRD) patterns. With decreasing x-value, the phase compositions systematically changed from α'_{L} and INC ($0.125 \leqslant x \leqslant 0.150$), α'_{L} ($0.105 \leqslant x \leqslant 0.11$), β and α'_{L} ($0.075 \leqslant x \leqslant 0.10$) to β ($x \leqslant 0.065$) [18]. Because the α'_{L}-to-β transformation is martensitic, the amount of transformation has been dependent not only on the x-value but also on physical effects such as the size of the crystal grains and the intensity of the thermal stress on quenching [19]. At ambient temperature, the relative amount of β with respect to α'_{L} was changed most significantly for the crystals with $x = 0.09$.

The hydraulic activities evaluated by compressive strength development were reported to be higher for the β-phase than for the α'-phase, the P_2O_5 contents of which were 2.3% ($x = 0.056$) and 7.6% ($x = 0.181$), respectively [1]. The crystal surface of the β-phase ($0.022 \leqslant x \leqslant 0.088$) showed, when etched with a solution of nitric acid in alcohol, a higher density of etch pits than that of the α'-phase ($0.110 \leqslant x \leqslant 0.270$) [2]. Because the defects on the crystal surface usually behave like active centers for chemical reactions [20], one of the principal factors affecting hydraulic activity would be the defect state, such as type and concentration of defects [2].

---

* Corresponding author. Tel.: 81-52-735-5289; Fax: 81-52-735-5294; E-mail: fukuda@mse.nitech.ac.jp.

PII: S0008-8846(98)00195-1

In the present study of the hydration of $C_2S(ss)$, we have, for the first time, fixed one of the most important variables, chemical composition, by taking advantage of the martensitic nature of the α'_L-to-β transformation. The powder specimens used for the hydration experiment were identical in chemical composition but different in phase composition. Because they showed almost the same particle size distributions as well as specific surface areas, the higher reactivity with water was ascribed to the more favorable defect state for the reaction with water.

1. Experimental

Crystals of $(Ca_{1.955}\square_{0.045})(Si_{0.91}P_{0.09})O_4$ were prepared from the reagent-grade chemicals of $CaCO_3$, SiO_2, and $CaHPO_4{\cdot}2H_2O$, where □ denotes a vacancy. The mixtures were, after calcination at 1200°C for 20 min, pressed into pellets (12 mm wide and 3 mm thick), heated at 1500°C for 3 days, and quenched in cold water (sample S-1). Part of the sintered pellets thus obtained was ground using a planetary micromill (model P-7, Fritsch, Idar-oberstein, Germany), reheated at 600°C (stable temperature region of the α'_L-phase) for 5 min, followed by quenching in air (S-2). Both samples were ground and sieved to obtain fine powder specimens with narrow size fractions.

Polished and thin sections were prepared for both samples and the microtextures were observed using an optical microscope.

The phase composition was examined using an X-ray powder diffractometer (model PW3050, Philips Analytical X-Ray B.V., Almelo, The Netherlands). The profile data were collected using monochromatized CuKα radiation (50 kV, 40 mA) and a step-scan technique (step width = 0.02° and fixed time = 5 s) in the 2θ range from 30° to 35°. Individual scale factors of the α'_L- and β-phases were refined by a whole-powder-pattern fitting without reference to a structural model method [21]. According to the quantitative phase-analysis procedure in previous studies [19,22], the molar fractions of the α'_L- and β-phases were deduced from the scale factors.

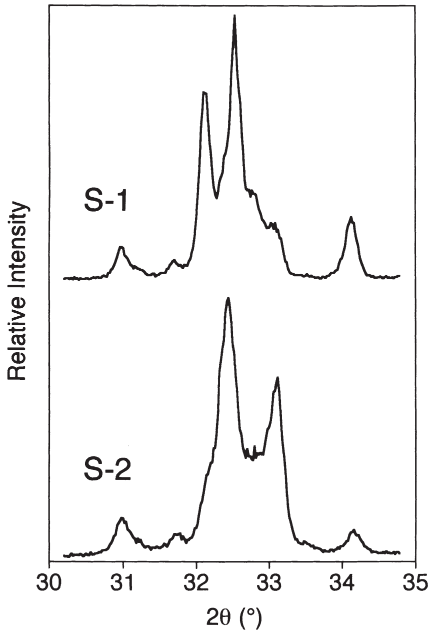

Fig. 1. Powder XRD patterns of samples S-1 and S-2. S-1 is composed of 30% α'_L and 70% β, and S-2 is composed of 92% α'_L and 8% β. The chemical compositions of both samples are exactly the same and the formula is represented by $(Ca_{1.955}\square_{0.045})(Si_{0.91}P_{0.09})O_4$.

The particle size fractions were measured using a laser granulometer (model LA500, Horiba Co., Tokyo, Japan). The specific surface area was examined using a BET three-point method (model NOVA1000, Yuasa Ionics Co., Osaka, Japan). Each powder specimen (20.0 g) was mixed with distilled water (water-to-sample ratio = 0.4 in weight) in a conduction calorimeter (model TCC-23, Tokyo Rikou Co., Tokyo, Japan). The cumulative heat evolution at 20°C was measured for about 34 days. The accuracy was estimated to be within 3 J/g from the calibration made by electric heating.

Both samples were examined using a transmission electron microscope (TEM, model JEM 2000FX, JEOL, Ltd., Tokyo, Japan) operated at 200 kV and equipped with an energy-dispersive X-ray analyzer (EDS, model TN-5500, Traco Northern Inc., Middleton, WI). They were crushed between glass slides into fine powders and then deposited with ethyl alcohol on copper grids. Chemical analysis was made, together with selected area electron diffraction, for the same crystal fragments.

2. Results and discussion

2.1. Phase composition and powder property

From the XRD (Fig. 1), the phase compositions of samples S-1 and S-2 were found to be quite different from each other, in accordance with the previous study [19]. With S-1,

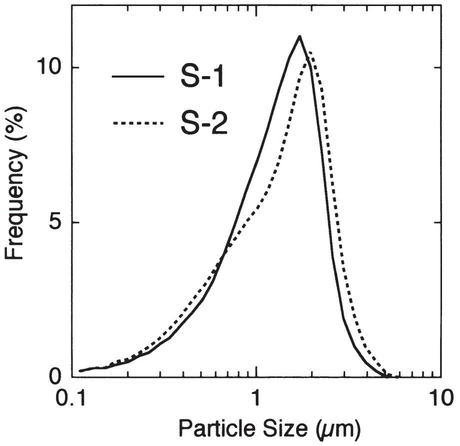

Fig. 2. Particle size fractions of powder specimens, the median sizes of which are 1.2 μm for S-1 and 1.3 μm for S-2. The particle size distribution was almost <3 μm.

the application of the thermal stress on quenching in water promoted the α'_L-to-β transformation. Thus, the sample was rich in the β-phase, the molar content of which was 70% (30% α'_L-phase). On the other hand, the transformation starting temperature of S-2 was lowered by reducing the grain size, which inhibited the transformation to the β-phase. Thus, the composition was 92% α'_L-phase and 8% β-phase. The EDS detected no difference in chemical composition, not only between samples S-1 and S-2 but also between the α'_L- and β-phases coexisting in each sample. This is in agreement with the nature of the martensitic transformation that the chemical compositions of the parent (α'_L) and the product (β) phases are identical with each other.

The pulverized specimens showed nearly the same specific surface areas (1.7 m^2/g for S-1 and 1.6 m^2/g for S-2) as well as very similar particle size fractions, the median sizes of which were 1.2 μm for S-1 and 1.3 μm for S-2 (Fig. 2). The particle size distribution was almost <3 μm for both specimens.

2.2. Hydration behavior

In the early stage of the hydration process, the powder specimen S-1 showed much higher hydraulic activity than S-2 (Fig. 3). After 3 days, the cumulative heat evolution of S-1 (40 J/g) was about eight times that of S-2 (5 J/g). After 15 days of hydration, however, both specimens showed almost the same cumulative heat of about 120 J/g. The heat evolution continued for 34 days, and the cumulative heat eventually reached 143 ± 3 J/g for both specimens.

The reaction that occurs in the early stage of the hydration process would be the interaction between the crystal surface and water, followed by the formation of hydrates. Because both specimens had almost the same powder properties (specific surface areas and particle size distributions) as well as identical chemical compositions, the higher reaction rate of specimen S-1 should be induced by the more favorable surface structure for the reaction with water.

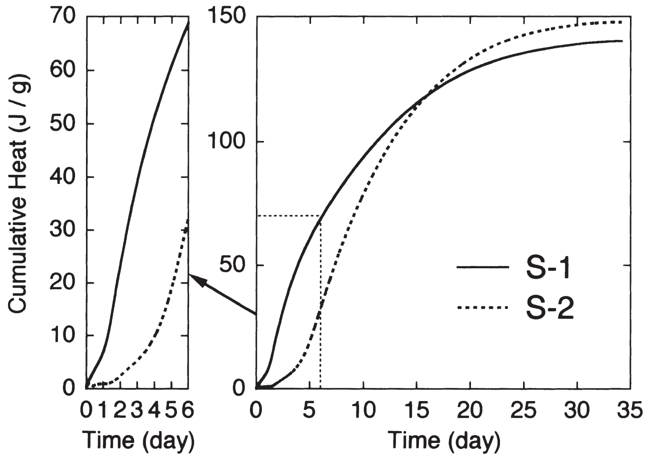

Fig. 3. Cumulative heat evolution of powder specimens. After 3 days of curing, the cumulative heat of S-1 (40 J/g) is about eight times that of S-2 (5 J/g). After 15 days of curing, both specimens have evolved almost the same cumulative heat.

Because the transformations $\alpha'_L \leftrightarrow \beta$ are martensitic and thus displacive, the differences in bulk crystal structure between the two phases are very small. This probably leads to almost the same eventual cumulative heat, in accordance with the present results.

2.3. Surface structures of the β-, α'_L-, and INC-phases

The present samples were quenched from the stable temperature region of the α-phase, hence they showed, under the optical microscope, the intracrystalline lamella structure induced by the α-to-α'_H phase transition [23,24]. However, the TEM analysis showed that the lamella structure was not observed within the crystal fragments of the pulverized specimens, because they were much smaller in size (<3 μm) than the individual lamellae. Accordingly, the lamella structure would have no influence on the hydration of both samples.

The β-phase crystal fragments showed the polysynthetic twinning on $(100)_\beta$ formed by the α'_L-to-β phase transition. The fragments were larger than the average twin width of about 100 nm to include large numbers of the twin domains and boundaries. For example, with the crystal fragment having a size of about 5 μm observed under TEM (Fig. 4), it contained about 50 twin boundaries. These boundaries, appearing as intersections on the crystal surface, would behave like active centers for the reaction with water. Due to their high density on the surface, the reactivity would be effectively increased. On the other hand, the crystal fragments of α'_L-phase were nearly uniform, with occasional line defects as observed in B_2O_3-doped α'-C_2S(ss) [4]. As a result, the hydration rate of the β-phase would be, during the early stage of the process, much higher than that of the α'_L-phase, leading to the higher cumulative heat evolution of the former phase.

The orthorhombic INC-phase appeared at ambient temperature when the trigonal α-phase failed to undergo the α-to-α'_H transition on rapid quenching [18]. The crystal grains consisted of domains related by a 120° rotation around the

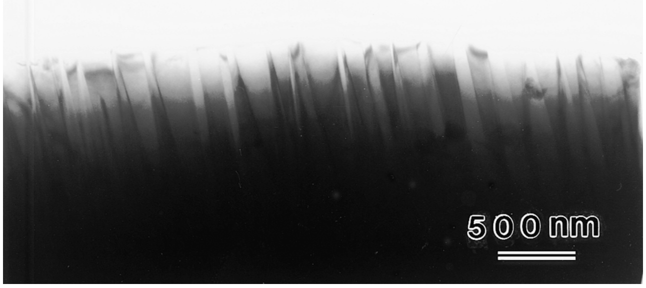

Fig. 4. TEM micrograph of a crystal fragment exclusively composed of the β-phase. Polysynthetically twinned on $(100)_\beta$. Sample S-1, bright-field image. The incident beam was nearly parallel to the b_β-axis.

former c_α-axis [16,17]. The domains were at the submicroscopic level and the boundaries were irregular. The domain sizes were much larger than the twin width of the β-phase, suggesting a much lower hydraulic activity than the β-phase.

3. Conclusions

Two types of powder specimens were prepared. They were exactly the same in chemical composition, $(Ca_{1.955}\square_{0.045})(Si_{0.91}P_{0.09})O_4$, although different in phase composition; one composition was 30% α'_L and 70% β and the other composition was 92% α'_L and 8% β.

With powder specimens of nearly the same specific surface areas and particle size distributions, the specimen rich in the β-phase showed, after hydration for 3 days, much higher hydraulic activity than that rich in the α'_L-phase.

The twin boundaries of the β-phase probably behaved on the crystal surface like active centers for the reaction with water, thus leading to the higher reactivity during the early stage of the hydration process.

After 15 days of hydration, both specimens showed nearly the same cumulative heat of about 120 J/g. The heat evolution continued for 34 days, with the eventual cumulative heat of 143 ± 3 J/g.

Acknowledgments

K. Fukuda is grateful to the Japan Cement Association for financial support.

References

[1] J.H. Welch, W. Gutt, Proc 4th Int Congr Chem Cem 1 (1960) 59.
[2] A.I. Boikova, M.G. Degen, V.A. Paramonova, Proc 6th Int Congr Chem Cem, Supplementary paper, I-3, 1974.
[3] M.Y. Bikbau, Proc 6th Int Congr Chem Cem, Supplementary paper, II-6, 1974.
[4] I. Jelenic, A. Bezjak, M. Bujan, Cem Concr Res 8 (1978) 173.
[5] K. Suzuki, S. Ito, S. Shibata, N. Fugii, Proc 7th Int Congr Chem Cem 2 (1980) 47.
[6] J. Skalny, J.F. Young, Proc 7th Int Congr Chem Cem 1 (1980) II-1/3.
[7] I. Jelenic, A. Bezjak, Cem Concr Res 11 (1980) 467.
[8] M.W. Barnes, M. Klimkiewicz, P.W. Brown, J Am Ceram Soc 75 (1992) 1423.
[9] H.F.W. Taylor, Cement Chemistry, second edition. Thomas Telford, London, 1997.
[10] R.L. Barrett, W.J. McCaughley, Am Miner 27 (1942) 680.
[11] R.W. Nurse, J.H. Welch, W. Gutt, J Chem Soc 220 (1959) 1077.
[12] W. Fix, H. Heymann, R. Heinke, J Am Ceram Soc 52 (1969) 346.
[13] H. Saalfeld, Z Kristallogr 133 (1971) 396.
[14] M.W. Barnes, M. Klimkiewicz, P.W. Brown, J Am Ceram Soc 75 (1992) 1423.
[15] H. Saalfeld, K.H. Klaska, Z Kristallogr 155 (1981) 65.
[16] K. Fukuda, I. Maki, J Am Ceram Soc 72 (1989) 2204.
[17] K. Fukuda, I. Maki, S. Ito, H. Yoshida, K. Aoki, J Am Ceram Soc 77 (1994) 2615.
[18] K. Fukuda, I. Maki, S. Ito, T. Miyake, J Ceram Soc Jpn 105 (1997) 117.
[19] K. Fukuda, E. Iizuka, H. Taguchi, S. Ito, J Am Ceram Soc 81 (1998) 2729.
[20] K. Sangwal, Etching of Crystals, North-Holland Physics Publishing, Elsevier Science Publishers B.V., Amsterdam, The Netherlands, 1987.
[21] H. Toraya, J Appl Crystallogr 19 (1986) 440.
[22] R.J. Hill, C.J. Howard, J Appl Crystallogr 20 (1987) 467.
[23] K. Fukuda, I. Maki, Cem Concr Res 19 (1989) 913.
[24] K. Fukuda, I. Maki, Cem Concr Res 23 (1993) 599.